Wettability evaluation of super-wetting surfaces coated with nanoparticles

Conference Paper · November 2016

CITATIONS
0

READS
98

4 authors:

Erivelto Santos
University of São Paulo
7 PUBLICATIONS **12** CITATIONS
SEE PROFILE

Francisco Do Nascimento
University of São Paulo
22 PUBLICATIONS **245** CITATIONS
SEE PROFILE

Debora Carneiro Moreira
University of São Paulo
27 PUBLICATIONS **274** CITATIONS
SEE PROFILE

Gherhardt Ribatski
University of São Paulo
204 PUBLICATIONS **3,474** CITATIONS
SEE PROFILE

WETTABILITY EVALUATION OF SUPER WETTING SURFACES COATED WITH NANOPARTICLES

Erivelto dos Santos Filho, erivelto.usp@gmail.com
Francisco Júlio do Nascimento, fnascimento@sc.usp.br
Debora Carneiro Moreira, dcmoreira@id.uff.br
Gherhardt Ribatski, ribatski@sc.usp.br
Heat Transfer Research Group, EESC-USP, Avenida Trabalhador São-carlense, 400, São Carlos - SP, 13566-590, Brazil

Abstract. *The present study concerns an investigation on the variation of wettability and roughness of flat aluminun plates covered with porous thin-films of nanoparticles. The contact angle of surfaces covered with a film of nanoparticles is near to 0, hence conventional methods are not suitable to evaluate the contact angle under this condition. Therefore, in the present study a new method was developed to evaluate the wettability. This method is based on the spreading velocity of a water droplet deposited on the surface. Aluminum oxide (20-30 nm) and silicon oxide (15 nm) nanoparticles were deposited on aluminum plates through a nucleate boiling process. The depositions were obtained through pool boiling of water/Al_2O_3 and water/SiO_2 nanofluids containing 0.01%, 0.1% and 0.5% in volume of nanoparticles. The roughness parameter R_t (maximum distance from peak to valley) increases with increasing volumetric concentration of the boiled nanofluid for both deposited materials. According to the wettability evaluation, two spreading mechanisms were identified, which are probably related to inertial and capillarity effects. In addition, it was noticed that droplets' spreading velocities on surfaces covered with SiO_2 increases with concentration, while no clear trend was recognized on surfaces covered with Al_2O_3 nanoparticles.*

Keywords*: Nanofluid, Nanoparticle, Roughness, Wettability, Critical Heat Flux.*

1. INTRODUCTION

Several important industrial applications rely on nucleate boiling to remove high heat fluxes from heated surfaces, like nuclear reactors, chemical reactors, electronic devices and solar power absorbers. Introducing nanoparticles into the base fluid is one way to improve the critical heat flux (CHF), as indicated by some studies in the literature (Ciloglu and Abduharrim, 2015; Kim, 2011), reaching up to 320% of CHF enhancement. The majority of these authors attribute the increase in CHF to the deposition of a layer of nanoparticles on the heated surface during the boiling process. This layer affects some of the surface's physical properties, changing the liquid-gas and solid surface tensions, as well as the contact angle (Vafaei et al., 2006, 2011). The deposition of nanoparticles can also alter the surface roughness (Chopkar et al., 2008; Narayan et al, 2007; Kim et al., 2008a,b) and wettability (Kim et al., 2008a,b, 2009). However, it is still not clear how these surface properties vary with changes in the characteristics of the boiled nanofluid, such as nanoparticles size, nanofluid concentration and boiling time.

The present work investigates how different materials and concentrations of nanoparticles deposited on flat aluminum plates through the boiling process can affect surface's roughness and wettability. Depositions of nanoparticles were obtained through pool boiling of water/Al_2O_3 (20-30 nm) and water/SiO_2 (15 nm) nanofluids for volumetric concentrations of 0.01%, 0.1% and 0.5%. Initial results demonstrated that the contact angle of surfaces covered with nanoparticles layer is near to zero. Due to the impossibility of evaluating the contact angle of superhidrophilic surfaces by usual methods, a new methodology was developed. This new approach is based on the spreading velocity of water droplet deposited on the surface coated with nanoparticles. The aim of this study is to evaluate the wettability on the surfaces covered with nanoparticles through a new perspective that can be described as how fast a water droplet spreads through the surface, especially for the first milliseconds.

2. EXPERIMENTAL APPARATUS AND PROCEDURE

2.1 Nanofluid preparation

All nanofluids were prepared according to the two-step method, which consists in adding the desired amount of nanoparticles into a suitable host liquid (DI-water for the present work) and homogenizing the solution. Due to high surface energy, agglomeration and clustering will easily appear. To minimize this effect and promote a homogenous dispersion, an ultrasonic homogenizer (ColeParmer CP505) was applied. According to Weng and Ding (2005) the average size of agglomerates and clusters rapidly decreases during the first 50 minutes of sonication. However, Motta (2012) concluded that the probe of the agitation equipment can be damaged due to cavitation phenomenon, and portion of it may also be dispersed into the nanofluid. In order to minimize this contamination, the agitation time adopted in the

present work was 30 minutes, resulting in a stable solution with a minimum period of ultrasonication time (Moraes, 2012).

Table 1 brings some characteristics of the nanoparticles purchased from Nanostructured & Amorphous Materials. The nanofluids were prepared for volumetric concentrations of 0.01%, 0.1% and 0.5%, using 300 ml of DI-water as host fluid. The digital balance employed to weight the nanoparticles was the Metler-Toledo AG245 with resolution of 0.0001 g, while the volume of DI-water was measured using a graduated beaker. The error associated with each concentration is 0.33%.

Table 1 – Nanoparticles characteristics.

Nanoparticles	Average particle size (nm)	Density (g/cm^3)	Purity (%)	Specific surface area (m^2/g)	Morphology
Al_2O_3	20-30 nm	3.7	99.97	180	Nearly spherical
SiO_2	15 nm	2.2-2.6	99.5	640	Spherical

2.2 Nanoparticles deposition

After ultrasonication, the nanofluid was transferred to the boiling system. The pool boiling procedure was set to 3 hours and it was performed in the apparatus shown in Fig.1, which consists of a bottom aluminum base (A) heated by a cartridge resistance of 245W (B), an aluminum plate (C), which is the plate where both boiling and deposition occur, a rubber disk (D) that seals the whole bottom part, a borosilicate glass tube (E) and the cooling aluminum block (F) attached to a cold water thermal bath, which to condenses the water vapor and maintains constant inner pressure and amount of liquid during the boiling process. After each deposition, the sample was stored and the system was cleaned up with water and acetone for preparing a new sample. To prevent contamination of the deposited surfaces, all samples were stored into a glass container wrapped in aluminum foil.

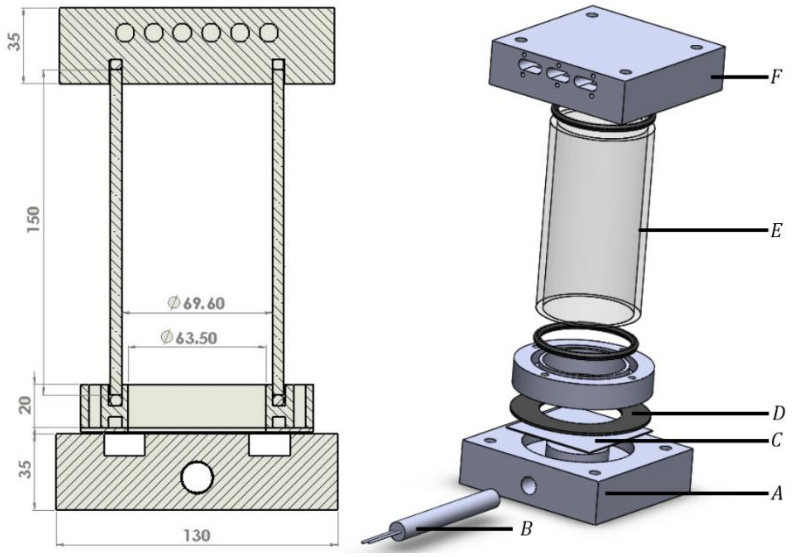

Figure 1 - The boiling apparatus (dimensions are in millimeters).

Three samples covered with alumina and three samples covered with silica were obtained after the deposition processes, one for each nanofluid containing different volumetric concentrations of nanoparticles. The deposited area is equal to 3167 mm^2, corresponding to a circle with a diameter of 63.5 mm. All samples were characterized according to their roughness and wettability.

2.3 Measurement of the surface roughness

Roughness measurements were performed using Veeco Wyko NT1100, providing 3D images of the surfaces with precision of 0.1 μm**.** All samples were evaluated at five different positions, each of them consisting of a square with 0.267 μm^2. Then an average roughness parameters were established for each sample as follows: average roughness across e measured area (R_a), root-mean-squared roughness (R_q), highest peak-to-valley difference (R_t), and average of the ten greatest peak-to-valley differences (R_z).

2.4 Wettability evaluation

The new wettability evaluation method is based on the analysis of images obtained from a DI-water droplet spreading through a horizontal flat aluminum plate coated with nanoparticles. The obtained images that reveal the wetted area by the DI-water were analyzed through the software ImageJ V. 1.48. Figure 2 shows the apparatus developed to measure the wettability, which consists of a flat horizontal surface where the sample must be allocated, a light source, a high speed camera (CamRecord 600) with lens AF MICRO NIKKOR 60mm and a micropipette. The camera was set to record images for 1s at 1000 frames per second with resolution of 1280x512 pixels. To ensure that the sample's surface was perpendicular to the camera, a digital inclinometer (DNM 60L Professional) with resolution of 0.1º was used. In order to obtain droplets with the same volume, an Eppendorf Research Plus micropipette was used, providing an error of 0.8%. Tests were performed for 8 µl because that was maximum volume that remained steady in the pipette tip without being released by gravitational force. The droplet was released with a small hand perturbation on the opposite side of the pipette. In order place the DI-water droplet in similar conditions on all surfaces, the distance between the surface and the needle tip was kept at 15 mm.

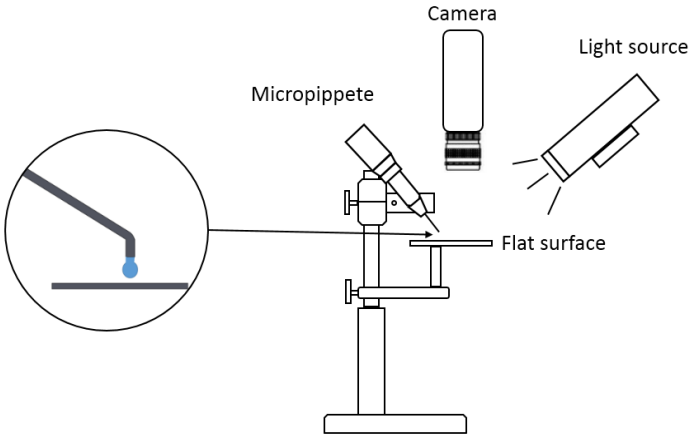

Figure 2 - Schematic of the experimental apparatus for wettability evaluation.

It was necessary to calibrate the image scale after setting up the apparatus in order to perform the tests. To calibrate the image scale, it is necessary to establish the mm/pixel ratio. A tape with known dimensions was placed on a flat aluminum surface (Fig. 3), with average width of 16.7 mm, corresponding an average of 517 pixels and resulting in a relation of 0.0323 mm/pixel.

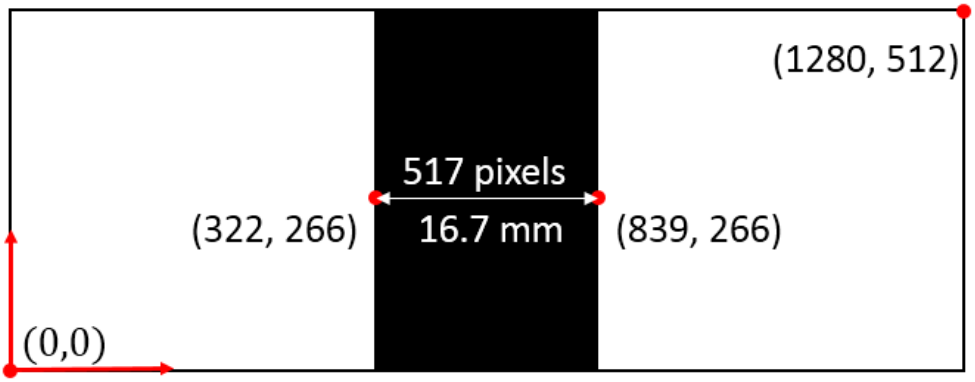

Figure 3 - Schematic picture to calibrate the camera and set the scale.

After placing a DI-water droplet on a deposited surface and obtaining the images of the wetting process, each image was analyzed and the wetted area measured in the software ImageJ V. 1.48. Besides the wetted area, the contact line velocity could also be calculated. The image parameters could be adjusted for a better contrast of the wetted area against the dry area, however, due to the non-uniformity of the deposition and needle interference, a phase detection software was unable to identify the wetted area, such that all areas were manually selected by the operator.

The method developed in the present study was validated by comparing the operator measurements against an image simulating a wetted area with known dimension. In order to verify if this method was capable of measuring precisely the area, the operator made 41 measurements. Results obtained are shown in Tab.2. To verify the significance

of these results, a t-student test with 95% confidence was applied in order to analyze if the measured area could be considered equal to the expected ones. Statistically, it was concluded that the data acquired by the method does not require any correction.

Table 2 - Results of the area measured simulating wetted area.

	Area (mm^2)	Standard deviation (mm^2)
Operator	33.068	0.082
Calculated	33.094	-

3. EXPERIMENTAL RESULTS AND DISCUSSION

3.1 Nanoparticles deposition

Figures 4 and 5 depict all obtained samples after the deposition of alumina and silica nanoparticles, respectively. These pictures evidence a visual non-uniformity of the nanoparticles' layers, especially in silica covered samples. According to Vafaei and Borca-Tasciuc (2014), the deposition of nanoparticles occurs preferentially near the active nucleation sites, which may explain the non-uniformities of the surface. In addition, large deteriorated areas, characterized by apparently uncovered regions, are identified in samples produced by the boiling process of nanofluids containing 0.5% of nanoparticles. This deterioration of the deposited porous layer of nanoparticles can be related to a possible detachment of nanoparticles after the layer reaches a maximum thickness. This behavior was noticed for different samples produced with nanofluids with 0.5% volumentric concentration.

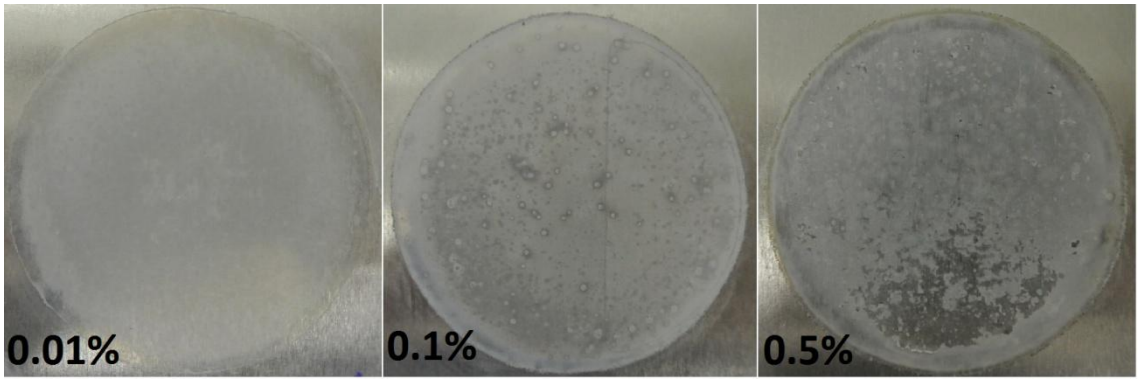

Figure 4 – Sample coated with γ -Al_2O_3 20 – 30 nm.

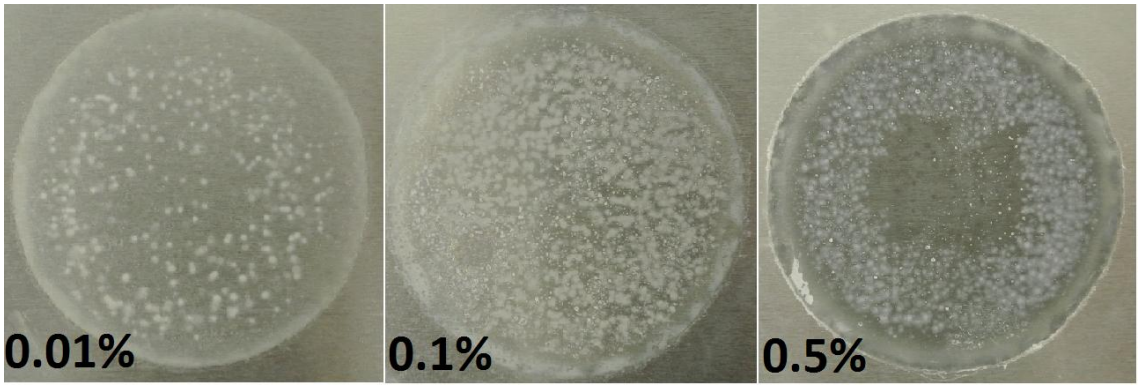

Figure 5 - Sample coated with SiO_2 15 nm.

3.2 Roughness results

Roughness of the samples was also measured, in order to identify the influence of the nanofluids concentration on the deposited porous layers. The profiles of the deteriorated regions were analyzed, corroborating the idea of a possible detachment of nanoparticles, as evidenced in Fig. 6, which shows the profilometry of this region from Al_2O_3 covered plates for volumetric concentration of 0.5%. The roughness of all samples was analyzed in different regions and compared to the roughness of the original aluminum plate. Table 3 presents roughness results of the deteriorated region of this sample, average values measured along the sample, and the results from the aluminum plate prior to the boiling

process. From this table, it is possible to conclude that the roughness from the deteriorated region is more similar to the surface before boiling than to the non-deteriorated region, strengthening the hypothesis of the detachment of the nanoparticles porous layer.

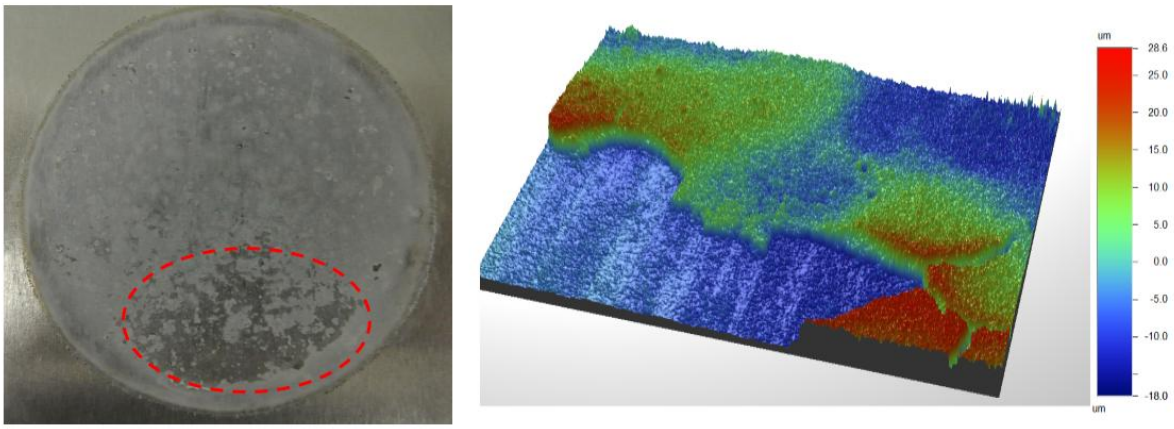

Figure 6 - Profilometry of the sample coated with Al_2O_3 20 – 30 nm obtained through the boiling process of a nanofluid with 0.5% volumetric concentration.

Table 3 - Roughness for different regions of the same Al_2O_3 20–30 nm 0.5% sample.

	Ra (nm)	Rq (nm)	Rz (μm)	Rt (μm)
Before boiling	570.76	711.39	4.17	4.47
Deteriorated region	827.27	1020	6.45	7.8
Sample	2030.0	2562.50	23.68	28.90

Roughness results of all samples are shown in Tab. 4, together with their respective standard deviations. For the surfaces coated with γ-Al_2O_3 nanoparticles the roughness seems to increase with rising volumetric concentration, while it is reasonable to say that samples covered with SiO_2 present no clear trend for changes in roughness with nanofluids concentration. It should be noted, however, that the standard deviation also rises significantly with concentration, revealing the non-uniformity of the deposited layers for the surfaces coated with γ-Al_2O_3.

Table 4 – Roughness before and after the deposition of nanoparticles.

Sample	Concentration (%)	R_a (nm)	σ (nm)	R_q (nm)	σ (nm)	R_t (μm)	σ (μm)	R_z (μm)	σ (μm)
Before boiling	-	570.76	-	711.39	-	4.5	-	4.2	-
$\gamma - Al_2O_3$ 20 − 30 nm	0.01	785.37	103.8	1017.3	147.7	17.8	2.1	13.1	2.7
$\gamma - Al_2O_3$ 20 − 30 nm	0.1	1118.5	306.5	1482.0	423.9	20.6	5.7	16.5	4.0
$\gamma - Al_2O_3$ 20 − 30 nm	0.5	2030.0	1081.3	2562.5	1322.3	28.9	5.2	23.7	4.1
SiO_2 15 nm	0.01	738.0	125.1	899.77	119.3	6.2	1.2	5.1	0.4
SiO_2 15 nm	0.1	709.89	20.1	888.12	44.7	8.4	2.5	7.2	2.7
SiO_2 15 nm	0.5	1000.1	199.3	1316.6	258.9	26.2	7.8	21.1	4.7

3.3 Evaluation of the wetted area

The static contact angle before the deposition of nanoparticle was 67.3° with 1.8° of standard deviation for 8 μl of DI-water. As already described, the wettability of the samples was analyzed according to the spreading velocity of a water droplet deposited on the surface. Figure 7 illustrates the evolution of the wetted area during the first 10 ms for the sample coated with Al_2O_3 for 0.1% of concentration in volume. During this period, the wetted area increased about 3.5 times. It is possible to observe that the wetted area presented a circular shape, and the apparent non-uniformities of this surface had no influence on the spreading behavior.

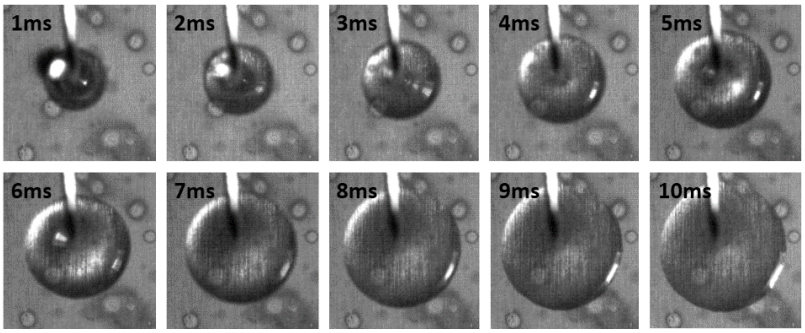

Figure 7 - Evolution of the wetted area for the sample coated with Al_2O_3 (20 – 30 nm) obatained from the boiling process of a nanofluid with 0.1% volumetric concentration. Frame rate of 1000 fps**.**

After the acquisition of the images of the spreading droplet on each sample, the evolution of the wetted area was evaluated. Figures 8 and 9 show this evolution for periods of 10 ms and 1000 ms for 8µl DI-water droplet right after the contact with the surfaces covered with **γ**-Al_2O_3 and SiO_2, respectively. The droplet quickly spread during the first 10 ms, and then it continues to grow at a lower rate on most samples.

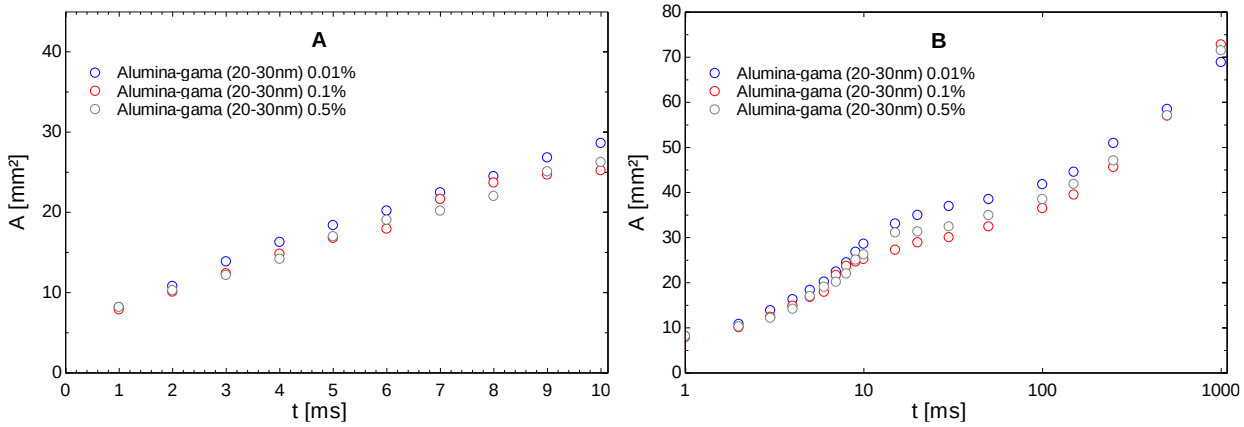

Figure 8 - Time evolution of the wetted areas for the surfaces coated with **γ** – Al_2O_3 (20 – 30 nm) during (a) the first 10 ms and (b) throughout the 1000 ms tests.

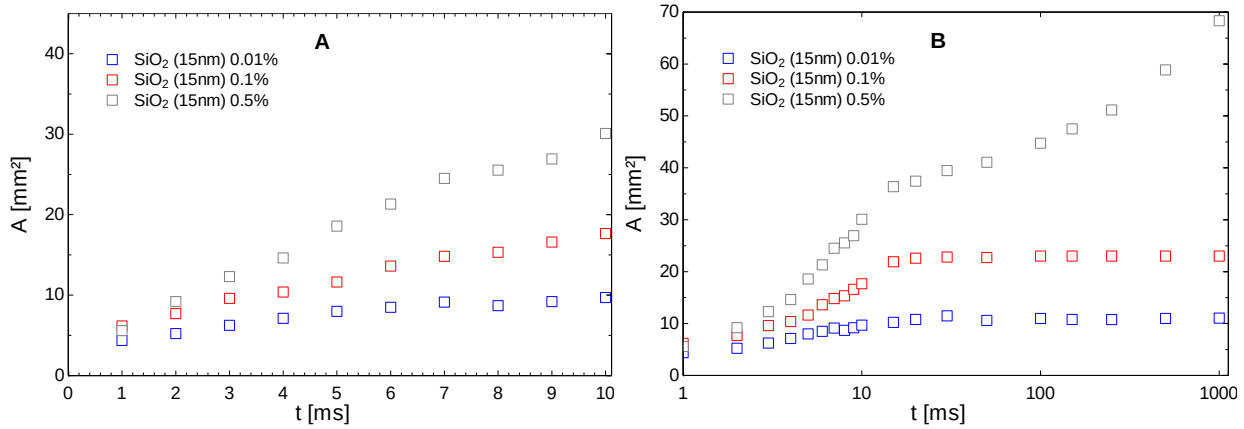

Figure 9 - Time evolution of the wetted areas for the surfaces coated with SiO_2 (15 nm) during (a) the first 10 ms and (b) throughout the 1000 ms tests.

For the surfaces coated with Al_2O_3, seen in Fig. 8, it is possible to notice that the spreading velocity does not depend on the concentration. Nevertheless, for the surfaces coated with SiO_2 nanoparticles the wetted area increases with increasing concentration. Also, the wetted areas on samples covered with lower concentrations of silica (0.01% and 0.1%) expand during the first milliseconds then stagnate, while wetted areas on all other samples continue growing. These results may indicate a change of mechanisms actuating in the spreading behavior, which could be mainly governed by inertial effects during the first 10 milliseconds and then by capillarity effects, due to the porous layer. The average spreading velocity of the contact line was calculated considering the radius variation of circles with areas equal

to the measured wetted areas. In addition, due to the heterogeneous deposition of nanoparticles, the average spreading velocities in four different directions of the contact line were calculated for the first 10 ms as shown in the diagram in Fig.10.

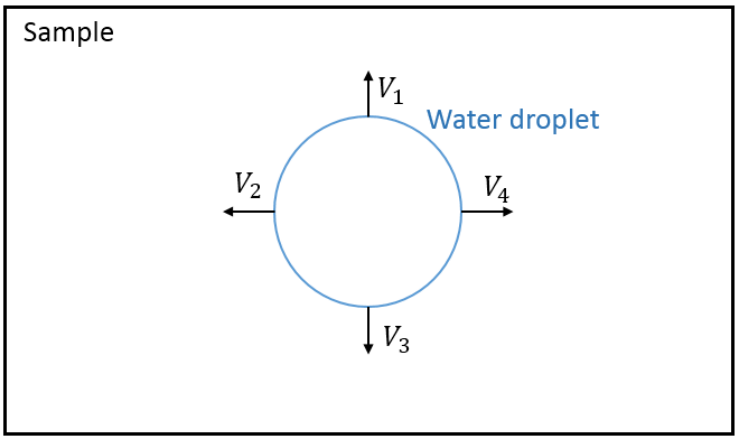

Figure 10 – Schematic diagram of the calculated spreading velocities at four different locations of the border of the water droplet.

Table 5 shows the calculated spreading velocities of the contact line of the water droplet in four different directions along with the average velocity, based on the measured area for all samples during the first 10ms. According to these results it is possible to analyze the homogeneity of the spreading droplet and possible influences of surface inhomogeneity in the wetting behavior. The error associated with the calculated velocities of the contact line is ± 0.02 mm/ms.

Table 5 - Average spreading velocities of the border of the water droplets for the first 10 ms on all samples.

Sample	Concentration (%)	$\overline{V_1}$ (mm/ms)	$\overline{V_2}$ (mm/ms)	$\overline{V_3}$ (mm/ms)	$\overline{V_4}$ (mm/ms)	$\overline{V}$ (mm/ms)	σ (mm/ms)
$\gamma - Al_2O_3$ 20 − 30 nm	0.01	0.312	0.276	0.307	0.294	0.297	0.016
$\gamma - Al_2O_3$ 20 − 30 nm	0.1	0.290	0.275	0.287	0.284	0.284	0.06
$\gamma - Al_2O_3$ 20 − 30 nm	0.5	0.284	0.289	0.291	0.283	0.286	0.04
SiO_2 15 nm	0.01	0.213	0.165	0.153	0.136	0.167	0.033
SiO_2 15 nm	0.1	0.223	0.214	0.273	0.222	0.233	0.027
SiO_2 15 nm	0.5	0.304	0.328	0.302	0.284	0.304	0.018

Visual observations of the shape of the water droplet spreading along the surfaces coated with aluminum oxide for all concentrations and silicon oxide for 0.5% in volume fraction showed nearly circular spreading droplets. This behavior can be confirmed by the calculated contact line velocities, which are similar for the four directions. Samples coated with silicon oxide for 0.01 and 0.1% concentrations, however, presented preferential spreading directions that were identified in the experiments due to non-circular shape of the spreading droplets. It can be speculated that the silicon oxide porous layer became more homogeneous and hydrophilic with higher concentrated nanofluids, thus increasing the wetted area and also intensifying capillarity effects.

4. CONCLUSIONS

This study demonstrates that pool boiling of nanofluids has a great potential to modify some properties of metallic surfaces due to the deposition of nanoparticles, consequently creating porous layers that modify the surfaces' wettability. Due to the impossibility of measuring contact angles close to zero by conventional methods, a new method was developed based on the spreading velocity of a DI-water droplet along the surface. The main findings of this study are summarized as follows:

- The deposition of nanoparticles on a surface through pool boiling of nanofluids turned the original aluminum plates into super-wetting surfaces, independently of the employed nanoparticles or concentrations of the boiled nanofluids.
- The surface roughness of all samples has increased with the deposition of nanoparticles, and was slightly higher for higher concentrations of the nanofluids.

- Two mechanisms were identified for the observed spreading behavior, with inertial effects governing during the first milliseconds and capillarity effects acting to further spread the droplets.
- For samples coated with SiO_2 (15 nm) nanoparticles, the spreading velocity of the droplet increased with rising nanofluid concentration applied in the boiling process, which is probably related to the non-uniformity of the porous layer on samples obtained with lower concentrated nanofluids.
- Samples coated with Al_2O_3 (20-30 nm) were visually more homogeneous than SiO_2 covered plates, and no significant changes in spreading velocity could be observed according to the concentration of boiled Al_2O_3 nanofluids.
- The shapes of spreading water droplets were nearly circular for all samples coated with aluminum oxide and for the silicon oxide with 0.5% concentration. However, for the samples coated with silicon oxide obtained from the boiling process of nanofluids containing 0.01 and 0.1% of concentration, the water droplet did not assume a regular shape and rapidly reached their maximum wetted areas.

5. ACKNOWLEDGEMENTS

The authors gratefully acknowledge the financial support provided by NANOBIOTEC-CAPES, FAPESP (2011/13119-0) and CNPq (404437/2015-0). The technical support given to this investigation by Hélio Donisetti Trebi and professor Renato Goulart Jasinevicius also appreciated and deeply recognized.

6. REFERENCES

CHOPKAR, M.; DAS, A. K.; MANNA, I.; DAS, P. K. Pool boiling heat transfer characteristics of ZrO2–water nanofluids from a flat surface in a pool. Heat and Mass Transfer, v. 44, n. 8, p. 999–1004, 2008.

CILOGLU, D.; ABDUHARRIM, B.; A comprehensive review on pool boiling of nanofluids. Applied Thermal Engineering, v. 84, p. 45-63, 2015.

KIM, H. Enhancement of critical heat flux in nucleateboiling of nanofluids: a state-of-art review. Nanoscale Research Letters, v. 6, 2011.

KIM, S. J.; MCKRELL, T.; BUONGIORNO, J.; HU, L. Alumina Nanoparticles Enhance the Flow Boiling Critical Heat Flux of Water at Low Pressure. v. 130, n. April, p. 18–20, 2008a.

KIM, S. J.; MCKRELL, T.; BUONGIORNO, J.; HU, L. Experimental Study of Flow Critical Heat Flux in Low Concentration Water-Based Nanofluids. Journal of Heat Transfer. v. 130, p. 599-603, 2008b.

KIM, S. J.; MCKRELL, T.; BUONGIORNO, J.; HU, L. Experimental Study of Flow Critical Heat Flux in Alumina-Water, Zinc-Oxide- Water, and Diamond-Water Nanofluids. Journal of Heat Transfer. v. 131, n. April, p. 1–7, 2009.

MORAES, A. A. U. Avaliação teórica e experimental do coeficiente de transferência de calor e do fluxo crítico durante ebulição convectiva de nanofluidos. Relatório final de Pós-Doutorado. Escola de Engenharia de São Carlos. Universidade de São Paulo. São Carlos. 2012.

MOTTA, F. C. Caracterização da condutividade térmica, viscosidade dinâmica e ângulo de contato de nanofluidos baseados em particulas de alumina-gama em água. Dissertação de Mestrado. Escola de Engenharia de São Carlos. Universidade de São Paulo. São Carlos. 2012.

NARAYAN, G. P.; ANOOP, K. B.; DAS, S. K. Mechanism of enhancement / deterioration of boiling heat transfer using stable nanoparticle suspensions over vertical tubes. Journal of Applied Physics, v. 074317, n. 2007, 2015.

VAFAEI, S.; BORCA-TASCIUC, T.; PODOWSKI, M. Z.; PURKAYASTHA, A. .; RAMANATH, G.; AJAYAN, P. M. Effect of nanoparticles on sessile droplet contact angle. Nanotechnology, v. 17, p. 2523–2527, 2006.

VAFAEI, S.; WEN, D. Flow boiling heat transfer of alumina nanofluids in single microchannels and the roles of nanoparticles. Journal Nanopart Res. v. 13, p. 1063–1073, 2011.

VAFAEI, S., BORCA-TASCIUC, T. Role of nanoparticles on nanofluid boiling phenomenon: Nanoparticle deposition. Chemical Engineering Research and Design v. 92, p. 842–586, 2014.

WEN, D.; DING, Y. Formulation of nanofluids for natural convective heat transfer applications. International Journal of Heat and Fluid Flow, v. 26, n. 6, p. 855–864, 2005.

7. RESPONSIBILITY NOTICE

The authors are the only responsible for the printed material included in this paper.